Journal University of Kerbala , Vol. 16 No.1 Scientific . 2018

Comprehensive Faults Classification Method for Unbalanced Power Distribution Systems

طريقة تصنيف الاعطال الشاملة لأنظمة توزيع القدرة الكهربائية غير المتوازنة

Dr. Shamam Fadhil Alwash
Department of Electrical Engineering, College of Engineering, University of Babylon, Babylon, Iraq
shamamalwash@ieee.org

Abstract:

Unbalanced power distribution systems experience single faults and compound faults types. The classification of these faults is considered as one of the most important requirements for the fault analysis and the fault location techniques. However, existing methods for fault classification have been formulated to consider only single-fault types. This paper presents a comprehensive faults classification method for unbalanced power distribution systems. In this method, new fault classification indices are derived to consider all fault types including the compound-fault ones. The values of these indices are determined based on the transient analysis of the current signals using discrete wavelet transform (DWT). These indices are utilized in conjunction with adaptive neural-fuzzy inference systems (ANFIS) to classify all fault types. In order to verify the accuracy of the proposed method, a practical distribution system is used to test the method under different fault conditions.

Keywords: adaptive neural-fuzzy inference systems (ANFIS), discrete wavelet transform (DWT), distribution systems, fault type classification, unbalanced power systems.

الخلاصة:

تتعرض انظمة التوزيع غير المتوازنة بشكل مستمر الى انواع اعطال مفردة و مركبة. ان تصنيف هذه الاعطال هو أحد أهم متطلبات تحليل الاعطال وتقنيات تحديد مواقع الاعطال. ومع ذلك، فقد ركزت الطرق الموجودة الحالية لتصنيف الاعطال على انواع الاعطال المفردة فقط. يقدم هذا البحث طريقة شاملة لتصنيف الأعطال في أنظمة توزيع القدرة غير المتوازنة. في هذه الطريقة، تم اشتقاق مؤشرات تصنيف اعطال جديدة والتي يمكن من خلالها تصنيف جميع أنواع الاعطال بما في ذلك الاعطال المركبة. ان قيم هذه المؤشرات تحدد بالاستناد الى تحليل العابر لإشارات التيار باستخدام تحويل المويجات المنفصل (DWT). وتستخدم هذه المؤشرات بالاقتران مع أنظمة الاستدلال العصبي الضبابي التكيفية (ANFIS) لتصنيف جميع أنواع الاعطال. من اجل اثبات دقة الطريقة المقترحة يستخدم في هذا البحث نظام توزيع عملي لاختبار الطريقة المقترحة في ظل ظروف اعطال مختلفة.

الكلمات المفتاحية: أنظمة الاستدلال العصبي الضبابي التكيفي (ANFIS)، تحويل المويجات المنفصلة (DWT)، أنظمة التوزيع، تصنيف نوع العطل، انظمة القدرة غير المتوازنة.

I. Introduction

The classification of the fault type represents the main requirement for the fault analysis as well as for determining its location. Generally, different fault types have different formulation analysis and fault location equations [1]. Thus, correct fault analysis and accurate fault location can only be obtained if the fault type is accurately classified [2].

Accordingly, many methods were proposed to classify the fault type in power transmission systems [3]. These methods can be categorized into two groups. The methods of the first group classify the fault type based on the analysis of the symmetrical components or phase components determined from the measured signal at the sending-end of the transmission line [4-6]. In the second group, the transient current signal, measured at one-end or two-ends of the transmission line, are analyzed using discrete wavelet transform (DWT) or Hilbert transform to extract features for each fault type. These features are then utilized to classify the fault type [7-9]. However, all of these

methods assumed that the system is balanced and the measurements are available at each transmission line.

Recently, most distribution systems have been expanded to cover large geographical area due to the increase in population and urbanization. Consequently, locating the fault in distribution systems by using on-site inspection techniques became more difficult, especially in the case of underground cables. In order to decrease the outage time and the inspection cost, automated fault location techniques have been wildly used in the distribution systems [10]. The most important requirement of these techniques is the accurate classification of the fault type. It is worth mentioning that fault type classification (FTC) methods proposed for transmission systems are not efficient for distribution systems due to some special characteristics of distribution systems such as; the tree topological structure, the unbalanced operation and the availability of measurement only at substation bus. Thus, it is very important to develop a FTC method which takes the special characteristics of distribution systems into account.

Several FTC methods were proposed to classify the fault type in power distribution systems. A FTC method, based on the symmetrical components of the fundamental fault current and fuzzy logic, is proposed in [11]. In this method, the discrete Fourier transform was used to determine the fundamental current from the transient fault current signal measured at substation bus. The measurement of the transient voltage signal is also required to determine the angular differences between the voltage and current signals. However, this method suffers from inaccuracy due to the effects of the exponentially decaying DC-component of the signal on the determination of the fundamental fault current [1].

In order to avoid the inaccuracy due to the utilization of the fundamental fault current, many FTC methods, based on the analysis of the transient fault current signals, have been developed [12, 13]. In these methods, features which were directly extracted from the transient fault signals using DWT, are used for the classification. In order to get fast and accurate decision, other researches classify the fault type using the combination of the DWT and a classification technique such as fuzzy logic [14, 15], artificial neural networks [16] and adaptive neural-fuzzy inference systems (ANFIS) [17].

However, all of the mentioned methods are formulated for single-fault types while the compound fault types have not been considered. This drawback will adversely affect the fault analysis accuracy as well as the efficiency of the fault location techniques [1, 2]. In this paper, a fault classification method, based on DWT and ANFIS algorithm, is proposed. The transient current signals, captured at the substation bus, are only required to classify the single-fault and the compound-fault types in unbalanced power distribution systems.

II. Proposed Fault Classification Method

The proposed method classifies the single-fault types and the compound-fault types in unbalanced power distribution systems using four steps as shown in Figure (1). In the first step, the pre-fault and the during-fault current signals are obtained for each phase and neutral of the substation bus. These signals are then analyzed, in the second step, using DWT. Based on the signals analysis results, the proposed fault classification indices are determined in the third step. In the final step, the proposed indices are utilized to classify the fault type by using the proposed ANFIS algorithm. Each step will be described as follows:

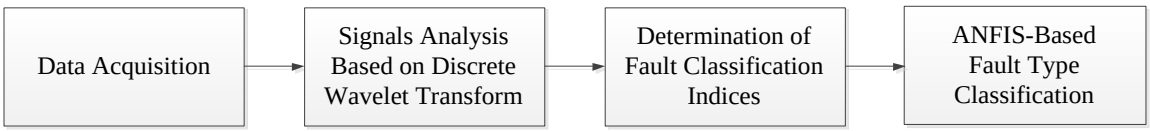

Figure (1): Block diagram of the proposed fault classification method

A. Data Acquisition

Once the fault occurs, the pre-fault and the during-fault current signals, measured at each phase of the substation bus, are recorded using digital fault recorders. The positive going zero crossing instant of the phase-a voltage is not recorded since the phase angle calculations are not required in the proposed method. The proposed fault recorder is designed to capture only one cycle of the pre-fault currents and one cycle of the during-fault current. A sampling rate of 10 kHz is utilized to convert the continuous signals to discrete signals. In order to minimize the storage memory of the digital recorder, the neutral current is calculated, instead of measured, using the following equations:

$$i_n^{pre} = i_a^{pre} + i_b^{pre} + i_c^{pre} \quad (1)$$

$$i_n^{dur} = i_a^{dur} + i_b^{dur} + i_c^{dur} \quad (2)$$

where i_a^{pre}, i_b^{pre} , i_c^{pre} and i_n^{pre} are the pre-fault currents for phase-a, phase-b, phase-c and neutral, respectively. i_a^{dur}, i_b^{dur} , i_c^{dur} and i_n^{dur} are the during-fault currents for phase-a, phase-b, phase-c and neutral, respectively.

B. Signals Analysis Based on Discrete Wavelet Transform

Usually, different fault types have different effects on the behavior of the fault current signals [1]. Thus, analyzing these signals can provide useful information to classify the fault type. Among many signals analysis tools, discrete wavelet transform (DWT) has recently showed a high efficiency tool for analyzing the transient signals in many power system applications [18].

Basically, DWT decomposes the discrete signal into components on different frequency bands. The DWT of a discrete signal is defined as [19]:

$$\mathrm{DWT(i,j)} = \mathrm{a_0}^{-\mathrm{i}/2} \sum_{\mathrm{k=1}}^{\mathrm{n}} \mathrm{X[k]}\ \psi\left[\frac{\mathrm{k} - \mathrm{j a_0^i\ b_0}}{\mathrm{a_0^i}}\right] \quad (3)$$

where a_0^i is a scale factor, $(ja_0^i\ b_0)$ is a time shift factor, i and j are integer numbers, $\psi[k]$ is the mother wavelet and n is the sample number of the original signal.

One of the best approaches of DWT is the multi-resolution analysis (MRA) [20]. In this approach, the discrete signal is decomposed into high frequency components (called details (D)) and low frequency components (called approximation (A)), with different resolution levels. The implementation of this approach is equivalent to successive pairs of low-pass and high-pass filters. The outputs of these filters represent the details and the approximation of the original signal for a specific resolution level.

Consider the block diagram, as shown in Figure (2), which represents the structure of two-level of the MRA approach. For the first-level, the discrete signal is passed through low-pass and high-pass filters, separately. The band-width of these filters is designed to be equal. The output signal of each filter is then down sampled or decimated by a factor of two to return the samples number of the output signals equal to those of the original signal. Accordingly, the frequency band of the high frequency component (D_1), which is obtained from the high-pass filter after decimating, is $(f_s/4\ \mathrm{Hz} - f_s/2\ \mathrm{Hz})$, where f_s is the sampling frequency. By the same manner, the frequency band of the low frequency component (A_1), which is obtained from the low-pass filter after decimating, is $(0\ \mathrm{Hz} - f_s/4\ \mathrm{Hz})$.

For the second level, the low frequency component (A_1), obtained from the first level, is broken down into high frequency component (D_2) and low frequency component (A_2) using another pair of low-pass and high-pass filters. Down sampling is also utilized in this level for the same reason mentioned above. Accordingly, the frequency band of $\mathrm{D_2}$ is $(\mathrm{f_s}/8\ \mathrm{Hz} - \mathrm{f_s}/4\ \mathrm{Hz})$ whereas the frequency band of $\mathrm{A_2}$ is $(0\ \mathrm{Hz} - \mathrm{f_s}/8\ \mathrm{Hz})$. The same decomposition processes can be used for other levels to obtain lower resolution components.

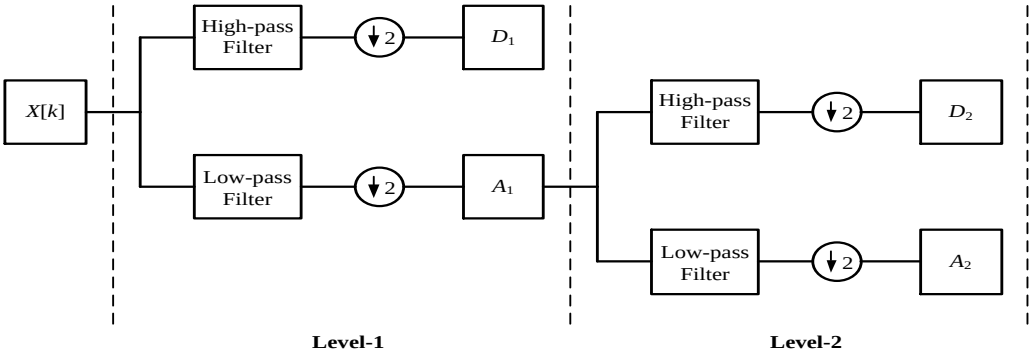

Figure (2): Structure diagram of the MRA approach

In this paper, the discrete electrical current signals, obtained from the first step of the proposed method (data acquisition), are analyzed using discrete wavelet transform. As mentioned before, the analyzed signals include the electrical current signals of the three phases and the neutral for the cases of the pre-fault and the during-fault periods. Four levels of the MRA approach are utilized to decompose these signals. The Daubechies-2 wavelet (db2) is selected as the mother wavelet. The energy (E) of the high frequency component obtained from the fourth level of the MRA approach (D_4) is determined for each signal using Equation (4):

$$E = \sum_{k} |D_4(k)|^2 \tag{4}$$

where $D_4(k)$ is the k^{th} sample of the D_4.

Accordingly, the energies of eight analyzed signals are determined in this section, and subsequently used in the next section to determine the fault classification indices.

C. Determination of Fault Classification Indices

In this step of the proposed method, seven indices are determined to classify the fault type in the power distribution system. The mathematical expressions for these indices are given as:

$$F_1 = 10^2 \cdot \left| \frac{E_a^{dur} - E_a^{pre}}{E_a^{dur}} \right| \tag{5}$$

$$F_2 = 10^2 \cdot \left| \frac{E_b^{dur} - E_b^{pre}}{E_b^{dur}} \right| \tag{6}$$

$$F_3 = 10^2 \cdot \left| \frac{E_c^{dur} - E_c^{pre}}{E_c^{dur}} \right| \tag{7}$$

$$F_4 = 10^2 \cdot \left| E_n^{dur} - E_n^{pre} \right| \tag{8}$$

$$F_5 = \frac{E_{ab} - \mu_n}{\mu_x - \mu_n} \tag{9}$$

$$F_6 = \frac{E_{bc} - \mu_n}{\mu_x - \mu_n} \tag{10}$$

$$F_7 = \frac{E_{ca} - \mu_n}{\mu_x - \mu_n} \tag{11}$$

Where F_i is the i^{th} fault classification index, E_ρ^{pre} is the energy of the high frequency component (D_4) for the case of the pre-fault current of the phase-ρ or the neutral, and E_ρ^{dur} is the energy of the high frequency component (D_4) for the case of the during-fault current of the phase-ρ or the neutral. E_{ab}, E_{bc}, E_{ca}, μ_n and μ_x are given as:

$$E_{ab} = \left|(E_a^{dur} - E_a^{pre}) - (E_b^{dur} - E_b^{pre})\right| \quad (12)$$
$$E_{bc} = \left|(E_b^{dur} - E_b^{pre}) - (E_c^{dur} - E_c^{pre})\right| \quad (13)$$
$$E_{ca} = \left|(E_c^{dur} - E_c^{pre}) - (E_a^{dur} - E_a^{pre})\right| \quad (14)$$
$$\mu_n = \text{Min}([E_{ab}\ E_{bc}\ E_{ca}]) \quad (15)$$
$$\mu_x = \text{Max}([E_{ab}\ E_{bc}\ E_{ca}]) \quad (16)$$

The first three indices represent the percentage of the energy difference between pre-fault and during-fault energies of a specific phase with respect to its during-fault energy. These indices are determined for the phases *a*, *b* and *c*, respectively. The forth index represents the energy difference between pre-fault and during-fault energies of the neutral. The main advantage of subtracting the pre-fault energy from the during fault energy is to eliminate the effect of harmonics produced due to the presence of nonlinear loads in the system and to consider only the effects of the faults on the proposed indices.

For all possible single fault types, the faulty phase can be identified according to the values of the indices F_1, F_2 and F_3 while F_4 is used to identify the ground fault type. Generally, the transient current signal of the faulty phase contains a dc-offsets component and multiple harmonic orders [1]. Thus, the during-fault energy of the faulty phase has a high value compared with the normal condition and the corresponding index will be also high. On the other hand, the during-fault energy of the healthy phase and the corresponding index will have low values. Similarly, the during-fault energy of the neutral current and the index F_4 have high values if an unbalanced fault is occurred, otherwise the values of the energy and the index will be low.

However, for the cases of the compound fault types; such as a AG fault combined with a BC fault, the four indices (F_1, F_2, F_3 and F_4) will have high values. Consequently, the fault is classified as compound fault type but the exact configuration cannot be determined (Which two phases are connected to each other? and Which phase is connected to ground?). In order to remedy this problem, the last three indices (F_5, F_6 and F_7) are proposed.

The indices (F_5, F_6 and F_7) represent the linearly normalized value of the energy difference between the two phases ab, bc and ca, respectively. The differences between the energies of the pre-fault and during-fault periods are also considered. These indices can help to identify the phase-to-phase faults in the compound fault types. As an example, if a fault is occurred between the phases a and b, the energies of these phases should be approximately equaled and the difference between them should be a low value. On the other hand, the value of the energy difference between any other phases should be high.

According to the aforementioned dissection, the proposed rules which are developed to classify all possible fault types are presented in Table (1).

However, it is very difficult to find the threshold value which differentiates between the ranges of low values and high values. Therefore, the fault type is classified, in this paper, using an ANFIS algorithm which has good classification ability even without the availability of the threshold value.

Table (1): Proposed fault classification rules

Single fault types							
Fault type	F_1	F_2	F_3	F_4	F_5	F_6	F_7
AG	High	Low	Low	High	-	-	-
BG	Low	High	Low	High	-	-	-
CG	Low	Low	High	High	-	-	-
ABG	High	High	Low	High	-	-	-
BCG	Low	High	High	High	-	-	-
CAG	High	Low	High	High	-	-	-
ABCG/ABC	High	High	High	Low	-	-	-
AB	High	High	Low	Low	-	-	-
BC	Low	High	High	Low	-	-	-
CA	High	Low	High	Low	-	-	-

Compound fault types							
Fault type	F_1	F_2	F_3	F_4	F_5	F_6	F_7
AG &BC	High	High	High	High	High	Low	High
BG & CA	High	High	High	High	High	High	Low
CG & AB	High	High	High	High	Low	High	High

D. ANFIS-Based Fault Type Classification

ANFIS is a fuzzy inference system whose membership function parameters have been tuned by using neural-adaptive learning methods [21]. The basic structure of ANFIS with two inputs is illustrated in Figure (3). It consists of five layers. In the first layer, fuzziness of inputs is determined based on the adaptive membership functions. Firing strength of each rule is determined in the second layer while their normalization is determined in the third layer. In the last two layers, the consequent parameters of the rule and fuzzy system output are determined, respectively.

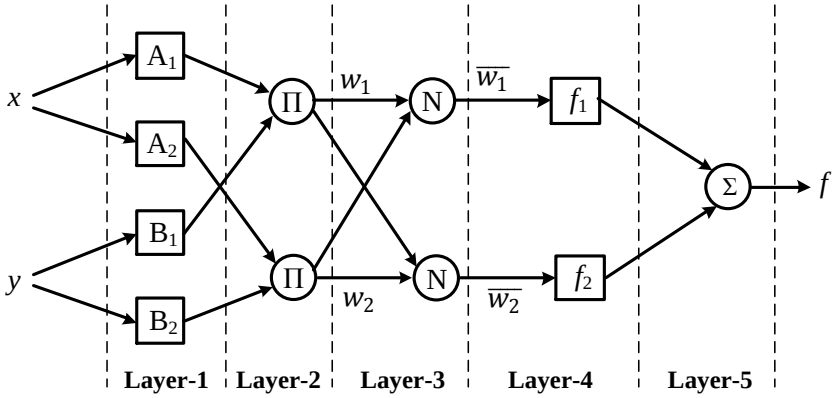

Figure (3): Basic structure of ANFIS

The ANFIS algorithm proposed in this paper is implemented in MATLAB environment. The seven classification indices, described before, are used as an input while the output refers to the fault type. The relations between the fault types and the approximate outputs of the ANFIS algorithm are presented in Table (2). Two membership functions are used for each input. The triangular membership function is selected. The thirteen rules illustrated in Table (1) are adopted in the proposed algorithm. The block diagram of the proposed ANFIS algorithm is presented in Figure (4). In the final stage of the ANFIS implementation, input and output patterns, for different fault conditions, are required to train and test the proposed algorithm.

Table (2): Approximate ANFIS output for each fault type

	Fault type	Approximate ANFIS output
Single-Fault type	AG	$1 \approx (1.5 > Out \geq 0.5)$
	BG	$2 \approx (2.5 > Out \geq 1.5)$
	CG	$3 \approx (3.5 > Out \geq 2.5)$
	ABG	$4 \approx (4.5 > Out \geq 3.5)$
	BCG	$5 \approx (5.5 > Out \geq 4.5)$
	CAG	$6 \approx (6.5 > Out \geq 5.5)$
	ABCG	$7 \approx (7.5 > Out \geq 6.5)$
	AB	$8 \approx (8.5 > Out \geq 7.5)$
	BC	$9 \approx (9.5 > Out \geq 8.5)$
	CA	$10 \approx (10.5 > Out \geq 9.5)$
Compound-Fault type	AG & BC	$11 \approx (11.5 > Out \geq 10.5)$
	BG & CA	$12 \approx (12.5 > Out \geq 11.5)$
	CG & AB	$13 \approx (13.5 > Out \geq 12.5)$

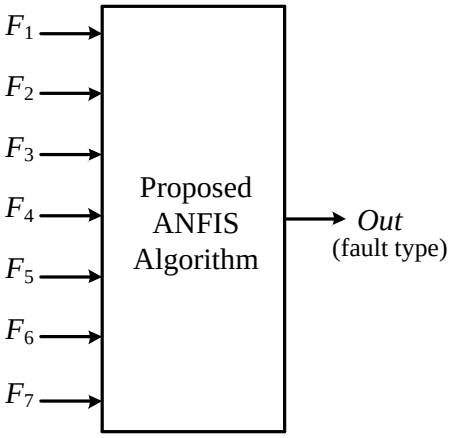

Figure (4): Block diagram of the Proposed ANFIS algorithm

III. Case Study

The case study, considered in this paper, is the IEEE 37-bus feeder, as shown in Figure (5). This system is an actual feeder located in California. It represents one of the best case studies provided by IEEE Power and Energy Society to evaluate the capability of the methods to handle the unbalanced characteristics of the distribution systems. The relevant data for this feeder are described in [22].

IV. Results and Discussion

In order to test the accuracy and the ability of the proposed method to classify all possible fault types including the compound-fault types, IEEE 37-bus feeder was simulated with PSCAD/EMTDC [23]. Simulations of different fault types with different fault and load conditions were carried out. For each simulation case, the pre-fault and during-fault current signals were recorded by using the PSCAD recorder and the proposed setting which is described in Section II.A. Figure (6) shows these signals for the case of an AG fault occurred at bus-737 with fault resistance of 0 ohm.

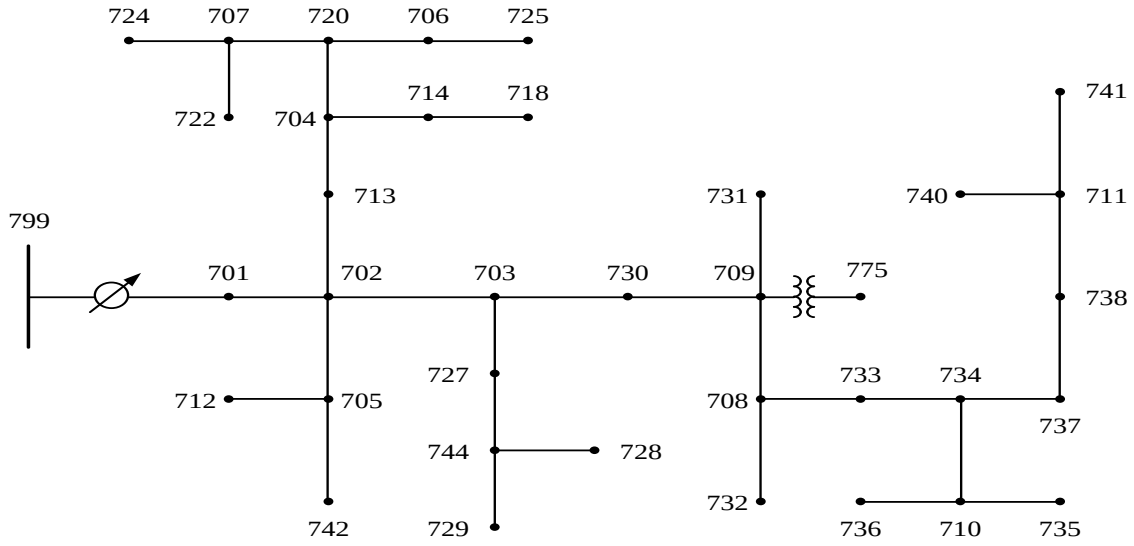

Figure (5): IEEE 37-bus feeder

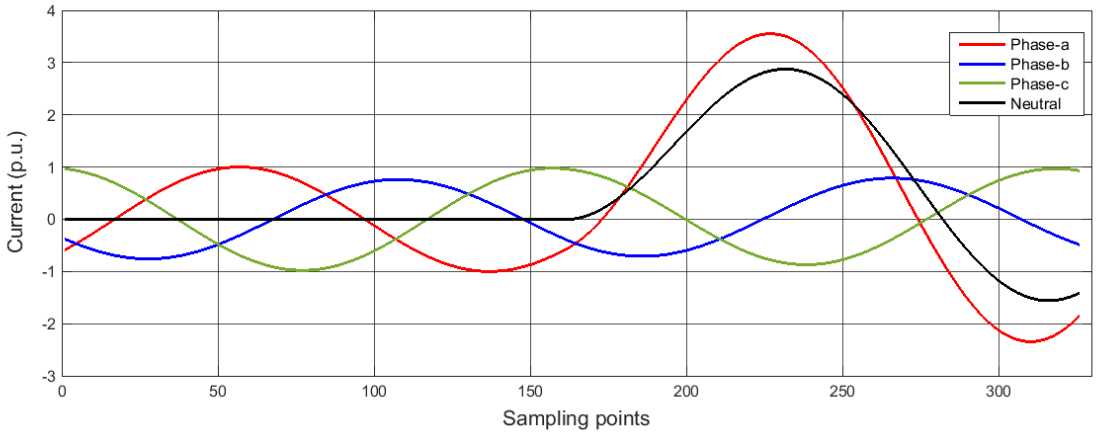

Figure (6): Pre and during fault current signals

The recorded signals were then exported to the MATLAB environment for analyzing by using DWT. From the analysis results, the proposed fault classification indices were determined and then used to train and test the proposed ANFIS algorithm.

In order to train ANFIS algorithm, simulations for ten fault locations, thirteen fault types, three fault resistances, five fault inception angles and three load conditions, as shown in Table (3), were carried out. It can be seen from the table that the fault resistances are assumed to be 0, 20 and 40 ohm. The fault inception angles (FIA) are -90^o, -30^o, 0^o, 30^o and 90^o whereas the load cases are assumed to be 25%, 50% and 100% from the base case of the system load. Due to the impossibility of listing all these data in this paper, samples of them are presented in Tables (4) and (5).

For the testing process, other simulation cases, as shown in Table (6), were carried out. In these cases, the variation of fault resistances, locations, inception angles and loads were considered. The total number of simulation cases for each fault type was 160.

Due to the space limitations of this paper, some of the testing results are illustrated in Table (7). In this table, the first five columns represent the fault type, fault location, fault resistance, FIA and load percentage of the simulation cases, respectively. The last column represents the output of the ANFIS algorithm. It can be seen form the table that the fault type is accurately classified for all illustrated cases. For the case of AG fault, the output of the ANFIS algorithm was 0.89 which is within the range of the AG fault type $(1.5 > Out \geq 0.5)$ that was presented in Table (2). In addition, for the case of CG fault combined with AB fault, the output was 12.68 which is also within the specified range $(13.5 > Out \geq 12.5)$.

In this paper, the classification accuracy for each fault type was determined using Equation (17) and the results were presented in Figure (7).

$$Accuracy = \frac{N_T - N_M}{N_T} \times 100 \qquad (17)$$

where;

N_T: Number of testing cases per fault type.

N_M: Number of testing cases per fault type which are misclassified.

It can be seen form Figure (7) that all fault types are accurately classified with an accuracy of 100% except the cases of ABG, BCG and CAG fault types. However, classification accuracies for these three types are 98.1%, 99.3% and 98.7%, respectively, which are still very high and acceptable for practical applications. In addition, the overall accuracy of the proposed method including all fault types is 99.7% where only 6 cases from 2080 cases are misclassified. These results verify the proposed method accuracy to classify the single and compound faults types in a practical system. Beside the accuracy, these results demonstrate the superiority of the proposed method over other methods which did not consider the compound-fault types.

V. Conclusions

A comprehensive faults classification method which is applicable for the single and the compound fault types in unbalanced power distribution systems, was proposed in this paper. This is in contrast with the existing methods which are formulated for only single types. Therefore, the proposed method is considered promising for practical applications. In the proposed method, four steps were used to classify the fault types. In the first step, proposed fault recorder was designed in PSCAD/EMTDC software to capture the transient current signals at the substation bus. These signals were analyzed, in the second step using DWT implemented in MATLAB. In the third step, novel fault classification indices were derived to consider all possible fault types. In the final step, the classification was obtained using proposed ANFIS algorithm. The proposed indices were used as the input to the algorithm while the output was the fault type. In order to test the proposed method, simulations for different fault conditions were carried out on a practical power distribution system. The results verified the accuracy and superiority of the proposed method over the existing methods.

Table (3): Different simulation cases for training process

Location (bus)	701, 703, 708, 724, 725, 729, 735, 737, 741, 742
Fault resistance (ohm)	0, 20, 40
FIA (deg.)	-90, -30, 0, 30, 90
Load (%)	25, 50, 100
Total simulation cases	5850

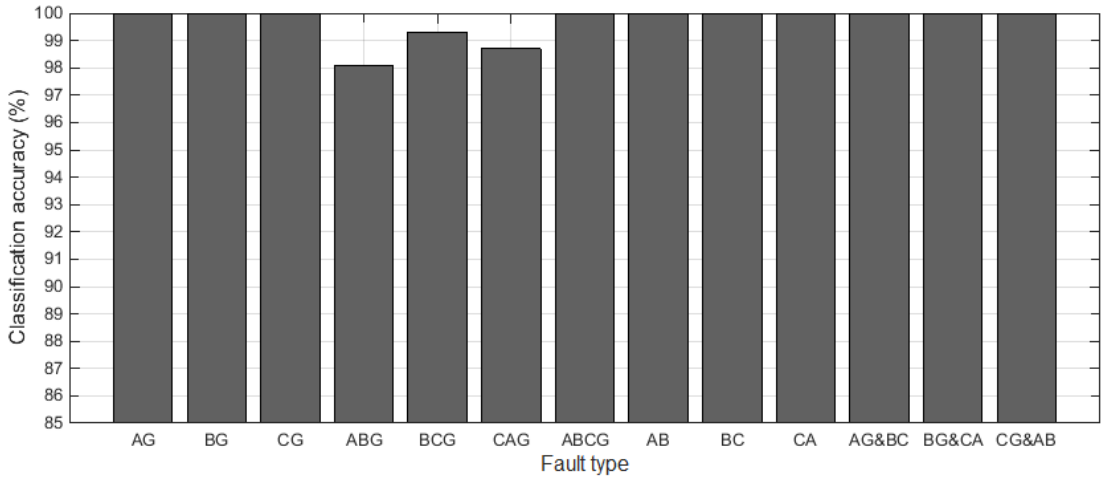

Figure (7): Fault classification accuracy

Table (4): Training sets for different faults occurred on bus-708 with 100% load, $R_F = 0$ ohm and FIA = -30^o

Fault type	F_1	F_2	F_3	F_4	F_5	F_6	F_7	Out
AG	64.19	2.37	5.61	4.13	0.96	0	1	1
BG	1.14	86.32	2.74	9.19	0.98	1	0	2
CG	0.38	6.08	67.57	6.34	0	1	0.98	3
ABG	96.72	98.23	1.85	2.08	0	1	0.91	4
BCG	0.91	98.64	97.41	1.41	1	0	0.85	5
CAG	92.98	0.95	94.14	3.00	0.82	1	0	6
ABCG	95.87	98.99	97.18	0	1	0.56	0	7
AB	97.01	98.01	4.06	0	0	0.85	1	8
BC	1.132	98.62	97.42	0	1	0	0.86	9
CA	92.71	6.480	94.12	0	0.78	1	0	10
AG & BC	62.38	98.60	97.45	4.58	1	0	0.89	11
BG & CA	92.80	85.96	94.03	9.32	0.74	1	0	12
CG & AB	96.97	98.08	69.27	6.31	0	0.91	1	13

Table (5): Training sets for different faults occurred on bus-741 with 50% load, $R_F = 40$ ohm and FIA = 90^o

Fault type	F_1	F_2	F_3	F_4	F_5	F_6	F_7	Out
AG	42.19	0.47	0.01	0.82	0.99	0	1	1
BG	5.81	58.51	4.02	0.97	0.86	1	0	2
CG	2.43	0.84	45.83	1.26	0	0.97	1	3
ABG	30.21	62.29	0.15	0.63	0.16	1	0	4
BCG	1.87	68.04	67.11	0.47	0.40	0	1	5
CAG	59.58	1.35	54.97	0.72	1	0.75	0	6
ABCG	46.88	68.35	69.00	0	0	0.59	1	7
AB	60.20	70.37	7.46	0	0	0.88	1	8
BC	1.36	80.20	70.90	0	0.99	0	1	9
CA	66.35	3.65	70.54	0	0.81	1	0	10
AG & BC	37.45	80.14	70.83	0.80	0.98	0	1	11
BG & CA	66.45	58.21	67.54	0.98	0.97	1	0	12
CG & AB	57.02	71.38	48.27	1.25	0	1	0.73	13

Table (6): Different simulation cases for testing process

Location (bus)	702, 704, 706, 710, 712, 722, 728, 731, 732, 740
Fault resistance (ohm)	5, 30
FIA (deg.)	-70, -10, 10, 70
Load (%)	40, 85
Total simulation cases	2080

Table (7): Classification results for different fault conditions

Fault type	Location (bus)	R_F (ohm)	FIA (deg.)	Load (%)	Out
AG	702	5	-70	40	0.89
BG	704	30	-10	85	1.97
CG	706	5	10	40	2.85
ABG	710	30	70	85	4.42
BCG	712	5	-70	40	4.87
CAG	722	30	-10	85	6.41
ABCG	728	5	10	40	7.25
AB	731	30	70	85	8.11
BC	732	5	-70	40	8.78
CA	740	30	-10	85	9.99
AG & BC	702	5	10	40	10.78
BG & CA	704	30	70	85	11.80
CG & AB	706	5	-70	40	12.68

References

[1] M. M. Saha, J. Izykowski, and E. Rosolowski, *Fault Location on Power Networks*. New York, USA: Springer, 2009.

[2] S. F. Alwash, V. K. Ramachandaramurthy, and N. Mithulananthan, "Fault-location scheme for power distribution system with distributed generation, " *IEEE Transactions on Power Delivery*, vol. 30, no. 3, pp. 1187–1195, 2015.

[3] V. H. Ferreira, R. Zanghi, M. Z. Fortes, G. G. Sotelo, R. B. M. Silva, J. C. S. Souza, C. H. C. Guimarães, and S. Gomes, "A survey on intelligent system application to fault diagnosis in electric power system transmission lines, " *Electric Power Systems Research*, vol. 136, pp. 135-153, 2016.

[4] T. Adu, "An accurate fault classification technique for power system monitoring devices, " *IEEE transactions on Power Delivery*, vol. 17, no. 3, pp. 684-690, 2002.

[5] M. M. Saha, E. Rosolowski, J. Izykowski, P. Pierz, P. Balcerek, and M. Fulczyk, "An efficient method for faulty phase selection in transmission lines," *IET International Conference on Developments in Power System Protection*, 2010.

[6] Q. Alsafasfeh, I. Abdel-Qader and A. Harb, "Symmetrical pattern and PCA based framework for fault detection and classification in power systems," *IEEE International Conference on Electro/Information Technology*, 2010.
[7] J.P.N. González, "Multiple fault diagnosis in electrical power systems with dynamic load changes using soft computing," *Mexican International Conference on Artificial Intelligence*, Springer, Berlin, Heidelberg, 2012.
[8] A. Prasad and J.B. Edward, "Application of Wavelet Technique for Fault Classification in Transmission Systems," *Procedia Computer Science,* vol. 92, pp. 78-83, 2016.
[9] N.R. Babu and B.J. Mohan, "Fault classification in power systems using EMD and SVM," *Ain Shams Engineering Journal*, vol. 8, no. 2, pp. 103-111, 2017.
[10] S. S. Gururajapathy, H. Mokhlis and H. A. Illias, "Fault location and detection techniques in power distribution systems with distributed generation: A review," *Renewable and Sustainable Energy Reviews*, vol. 74, pp. 949-958, 2017.
[11] B. Das, "Fuzzy logic-based fault-type identification in unbalanced radial power distribution system," *IEEE Transactions on Power Delivery*, vol. 21, no. 1, pp.278-285, 2006.
[12] A. M. El-Zonkoly, "Fault diagnosis in distribution networks with distributed generation," *Electric Power Systems Research*, vol. 81, no. 7, pp. 1482-1490, 2011.
[13] S. K. G. MukeshThakre and M. K. Mishra, "Distribution System Faults Classification and Location Based on Wavelet Transform," *International Journal on Advanced Computer Theory and Engineering*, vol. 2, no. 4, pp. 2319 – 2526, 2013.
[14] M. Jamil, R. Singh and S.K. Sharma, "ault identification in electrical power distribution system using combined discrete wavelet transform and fuzzy logic," *Journal of Electrical Systems and Information Technology*, vol. 2, no. 2, pp. 257-267, 2015.
[15] M. Dehghani, M.H. Khooban and T. Niknam, "Fast fault detection and classification based on a combination of wavelet singular entropy theory and fuzzy logic in distribution lines in the presence of distributed generations," *International Journal of Electrical Power and Energy Systems*, vol. 78, pp.455-462, 2016.
[16] M.S. ElNozahy, R.A. El-Shatshat and M.M.A. Salama, "Single-phasing detection and classification in distribution systems with a high penetration of distributed generation," *Electric Power Systems Research*, vol. 131, pp. 41-48, 2016.
[17] J. Zhang, Z.Y. He, S. Lin, Y.B. Zhang and Q.Q. Qian, "An ANFIS-based fault classification approach in power distribution system," *International Journal of Electrical Power and Energy Systems*, vol. 49, pp. 243-252, 2013.
[18] S. Avdaković and N. Čišija, "Wavelets as a tool for power system dynamic events analysis– State-of-the-art and future applications," *Journal of Electrical Systems and Information Technology*, vol. 2, no. 1, pp. 47-57, 2015.
[19] J. W. Lee, W. K. Kim, Y. S. Oh, H. C. Seo, W. H. Jang, Y. S. Kim, C. W. Park and C. H. Kim, "Algorithm for Fault Detection and Classification Using Wavelet Singular Value Decomposition for Wide-Area Protection," *Journal of Electrical Engineering and Technology*, vol. 10, no. 3, pp. 729-739, 2015.
[20] D. Sundararajan, *Discrete Wavelet Transform: A Signal Processing Approach*. John Wiley & Sons, 2016.
[21] F. Khoshbin, H. Bonakdari, S.H. Ashraf Talesh, I. Ebtehaj, A.H. Zaji and H. Azimi, "Adaptive neuro-fuzzy inference system multi-objective optimization using the genetic algorithm/singular value decomposition method for modelling the discharge coefficient in rectangular sharp-crested side weirs," *Engineering Optimization*, vol. 48, no. 6, pp. 933-948, 2016.
[22] W. H. Kersting, "Radial distribution test feeders," in *Proc. IEEE Power Eng. Soc. Winter Meeting*, vol. 2, pp. 908–912, 2001.
[23] *"PSCAD/EMTDC User's Manual,"* Manitoba HVDC Research Centre Inc., Winnipeg, MB, Canada, 2005.